

Three-Nucleon Continuum by means of the Hyperspherical Adiabatic Method

Paolo Barletta

*Department of Physics and Astronomy,
University College London, Gower Street, WC1E6BT London, UK*

A. Kievsky

*Istituto Nazionale di Fisica Nucleare,
Piazza Torricelli 2, 56100 Pisa, Italy*

Abstract

This paper investigates the possible use of the Hyperspherical Adiabatic basis in the description of scattering states of a three-body system. In particular, we analyze a 1+2 collision process below the three-body breakup. The convergence patterns for the observables of interest are analyzed by comparison to a unitary equivalent Hyperspherical Harmonic expansion. Furthermore, we compare and discuss two different possible choices for describing the asymptotic configurations of the system, related to the use of Jacobi or hyperspherical coordinates. In order to illustrate the difficulties and advantages of the approach two simple numerical applications are shown in the case of neutron-deuteron scattering at low energies using s -wave interactions. We found that the optimization driven by the Hyperspherical Adiabatic basis is not as efficient for scattering states as in bound state applications.

I. INTRODUCTION

The Hyperspherical Adiabatic (HA) method is based on the parametrization of the internal degrees of freedom with hyperspherical coordinates (see Refs.[1] and references therein). The method then consists in expanding the system's wavefunction on a basis made of hyperangular optimized functions (the adiabatic basis set) times (unknown) hyperradial functions. The hyperangular basis elements are taken as the eigenvectors of the Hamiltonian operator for a fixed value of the hyperradius ρ . Once those eigenvectors have been calculated, the hyperradial functions are obtained as the solutions of a system of coupled one-dimensional differential equations. The advantages of such approach are that the HA basis should drive a quick convergence for the expansion, due to its optimization, the payback is represented by the necessity and the difficulty in calculating accurately the first and second derivatives of the adiabatic basis set with respect to the hyperradius. Those terms are crucial to the method as they represent the coupling terms between the various hyperradial differential equations. In some applications of the HA method it was shown that the strong coupling between pair of elements of the adiabatic basis makes the hyperradial problem particularly hard to solve [2].

The properties of the adiabatic basis functions have been object of several studies and are well-known. In particular, in the asymptotic limit of large hyperradius the HA functions are known to converge towards the scattering states of the three-body system, both below and above break-up. This characteristic makes the adiabatic expansion a valid choice to describe the three-body continuum states. In the literature there are several studies of the bound spectrum of a three-nucleon system by means of the HA method [3, 4, 5], but very few dealing with continuum states [6]. This paper investigates the possibility of using the HA approach to describe a three-body elastic process in which a particle collides the other two, initially forming a bound state. The object of this work is the study of the appropriate boundary conditions to be imposed to the hyperradial functions as $\rho \rightarrow \infty$ and a careful analysis of the convergence properties of the HA expansion.

In order to quantitatively understand the pattern of convergence of the HA expansion we make use of the parallelism that can be built between the HA method and the Hyperspherical Harmonic (HH) expansion. In fact, we can consider two different expansions for the system's wavefunction, one in terms of N_A HA basis elements, and the second in terms of N_H HH basis

elements. When $N_A = N_H$ the two expansions are connected by a unitary transformation and therefore must yield identical results. Since the HH basis has been used several times to describe scattering states [7, 8], we exploit this knowledge to study the convergence of the HA expansion. In particular, we will study the convergence properties of the $L = 0$ phase shift at low energies in a $1 + 2$ collision, which has been used as a benchmark problem in literature (see for example [9]).

The problem of the boundary conditions to be imposed to the hyperradial functions is related to the difficulties associated with obtaining the eigenvectors and eigenvalues of the adiabatic Hamiltonian at large values of the hyperradius. As the lowest adiabatic functions tend to the two-body bound wavefunctions, an accurate description of those states using, for example, the expansion in HH functions is known to be very difficult. This is because, as $\rho \rightarrow \infty$, the two-body bound states are localized in a very small zone of the hyperangular phase-space. Consequently, this particular configuration necessitates a large number of HH functions to be described [2]. In fact, it can be shown that the number of HH required to reproduce this type of spatial configuration grows exponentially with the hyperradius. If the interest is limited to study deep three-body bound states, the problem just described does not manifest and a tractable number of HH functions suffices for a good accuracy. Due to the finite hyperradial size of the associated wavefunction, the adiabatic Hamiltonian needs to be solved only up to a non so large value of the hyperradius. However, there are cases in which shallow bound states are present (as Efimov states) and the adiabatic Hamiltonian needs to be solved for very large values of ρ . Furthermore, for energies in the continuum, the associated three-body scattering wavefunction has an infinite extension and a direct application of the HA necessitates of the solution of the adiabatic Hamiltonian at very large values of ρ , too. In order to obtain accurate asymptotic solutions to the adiabatic Hamiltonian we have followed in detail the procedure outlined by Nielsen and co-workers [1].

Finally, interest in this work is also sparked by an article of Fabre de la Ripelle [6], where he suggested the possibility of expanding the three-body asymptotic scattering states into the adiabatic basis set, and retaining only the first term in such an expansion, resulting in a considerable reduction of the numerical burden. We will analyze this truncation together with the contribution of higher terms.

This paper is organized as follows: in the next section the HA method is presented, by first introducing the notation. The expansion of the HA basis in terms of the HH functions

is given as well as the method to describe the HA functions and the adiabatic potentials at large values of ρ . Section III treats the problem of scattering states. Two different methods of implementing the Kohn Variational Principle are given in conjunction with the HA basis. The asymptotic conditions are given in terms of the distance between the incident particle and the two-body system and in terms of ρ . Section IV is devoted to numerical applications. Results are presented using a simple Gaussian two-body potential and the semi-phenomenological s -wave MT-III potential [10]. The final Section is devoted to the conclusions and perspectives.

II. HYPERSPHERICAL ADIABATIC METHOD

Let us consider a system of three identical particles of mass m , in a state of total orbital angular momentum $L = 0$. Other quantum numbers are represented by the total spin S , total isospin T , and the symmetry under particle permutation Π , which can take the values a (anti-symmetric, for three fermions) or s (symmetric, in the case of three bosons). A further quantum number needed to uniquely identify each wavefunction is given by the vibrational number n ($n = 1, 2, \dots$) for bound states or the energy E for continuum states.

Let us start from the definition of Jacobi coordinates $\{\mathbf{x}_i, \mathbf{y}_i\}$

$$\begin{aligned}\mathbf{x}_i &= \frac{1}{\sqrt{2}}(\mathbf{r}_j - \mathbf{r}_k) \\ \mathbf{y}_i &= \frac{1}{\sqrt{6}}(\mathbf{r}_j + \mathbf{r}_k - 2\mathbf{r}_i)\end{aligned}\tag{1}$$

where $\{\mathbf{r}_i\}$ are the Cartesian coordinates of the three particles and $i, j, k = 1, 2, 3$ cyclic. The hyperspherical variables $\{\rho, \theta_i\}$ are defined as follows

$$X_i = \rho \cos \theta_i, \quad Y_i = \rho \sin \theta_i\tag{2}$$

where ρ is the hyperradius which is symmetric under any permutation of the three particles and θ_i is the hyperangle, which is dependent on the particular choice of the Jacobi coordinate system. In terms of the interparticle distances $r_{ij} = |\mathbf{r}_i - \mathbf{r}_j| = \sqrt{2}X_k$ the hyperradius reads:

$$\rho = \frac{1}{\sqrt{3}}\sqrt{r_{12}^2 + r_{23}^2 + r_{31}^2}.\tag{3}$$

In addition to ρ and θ_i there are four more coordinates needed to parametrize all the possible spacial configurations of the three particles, for example the four polar angles which define

the orientation of the two Jacobi vectors with respect to the laboratory frame of reference. However, in the particular case of total orbital angular momentum $L = 0$, the number of such coordinates can be reduced to just one non-trivial functional dependence, represented by the cosine μ_i of the angle between the two Jacobi vectors $\{\mathbf{x}_i, \mathbf{y}_i\}$:

$$\mu_i = \mathbf{x}_i \cdot \mathbf{y}_i / (X_i Y_i). \quad (4)$$

In the following we will refer to the set of hyperangles $\{\theta_i, \mu_i\}$ as Ω_i , or more in general as $\Omega = \{\theta, \mu\}$ when there is no need to specify the choice of a particular permutation of the particles defining a set of Jacobi coordinates.

The Hamiltonian operator \mathcal{H} takes the following expression in hyperspherical coordinates

$$\mathcal{H} = -\frac{\hbar^2}{2m} T_\rho + \frac{\hbar^2}{2m\rho^2} G^2 + V(\rho, \Omega), \quad (5)$$

where V is the potential energy operator, T_ρ is the hyperradial operator

$$T_\rho = \frac{d^2}{d\rho^2} + \frac{5}{\rho} \frac{d}{d\rho} \quad (6)$$

and G^2 is the grand-angular operator

$$G^2 = \frac{4}{\sqrt{1-z^2}} \frac{d}{dz} (1-z^2)^{3/2} \frac{d}{dz} + \frac{\ell_x^2}{\cos^2 \theta} + \frac{\ell_y^2}{\sin^2 \theta}. \quad (7)$$

where $z = \cos 2\theta$ and ℓ_x and ℓ_y are the angular momentum operators associated with the \mathbf{x} and \mathbf{y} vectors, respectively. The volume element is $\rho^5 d\rho \sqrt{1-z^2} dz d\mu$.

The system wavefunction Ψ , with quantum numbers L, S, T, Π , and n (or E), is expanded as follows:

$$\Psi_n^{LST\Pi} = \sum_{\nu=1}^{\infty} u_\nu^n(\rho) \Phi_\nu^{LST\Pi}(\rho, \Omega), \quad (8)$$

where $\{\Phi_\nu^{LST\Pi}\}$ are the eigenfunctions of the operator \mathcal{H}_Ω made of the hyperangular part of the kinetic operator plus the potential energy operator, in which ρ acts only as a parameter:

$$\mathcal{H}_\Omega \Phi_\nu^{LST\Pi} = \left[\frac{\hbar^2}{2m\rho^2} G^2 + V \right] \Phi_\nu^{LST\Pi}(\rho, \Omega) = U_\nu(\rho) \Phi_\nu^{LST\Pi}(\rho, \Omega). \quad (9)$$

The set of eigenfunctions $\{\Phi_\nu^{LST\Pi}\}$ is known as the adiabatic basis set, and the associated eigenvalues $\{U_\nu(\rho)\}$ as the adiabatic curves or potentials. In practical calculations, the infinite expansion of eq. (8) needs to be truncated to a finite number of basis elements, say N_A . The convergence for the observables of interest with respect to this parameter is then checked.

The initial Hamiltonian problem is thus tackled in two steps: firstly, the HA basis functions $\{\Phi_\nu^{LST\Pi}\}$ and the associated potentials $\{U_\nu(\rho)\}$ are calculated by solving eq. (9). Secondly, the hyperradial functions $u_\nu^n(\rho)$ are obtained as the solutions of a system of N_A coupled one-dimensional differential equations, which can be expressed as follows [11]:

$$\sum_{\nu=1}^{N_A} \left[\left(-\frac{\hbar^2}{2m} T_\rho + U_\nu - E \right) \delta_{\nu'\nu} + B_{\nu'\nu} \right] u_\nu + C_{\nu'\nu} \frac{d}{d\rho} u_\nu + \frac{d}{d\rho} (C_{\nu'\nu} u_\nu) = 0 \quad (\nu' = 1, \dots, N_A), \quad (10)$$

where the coupling terms $B_{\nu'\nu}, C_{\nu'\nu}$ follow from the dependence on ρ of the HA basis :

$$B_{\nu'\nu}(\rho) = \frac{\hbar^2}{m\rho^2} \langle \frac{d\Phi_{\nu'}}{d\rho} | \frac{d\Phi_\nu}{d\rho} \rangle_\Omega, \quad (11)$$

and

$$C_{\nu'\nu}(\rho) = \frac{\hbar^2}{m\rho^2} \langle \Phi_{\nu'} | \frac{d\Phi_\nu}{d\rho} \rangle_\Omega. \quad (12)$$

For bound states solutions, and short range potentials, the functions $\{u_\nu\}$ tend to zero exponentially as $\rho \rightarrow \infty$, whereas for scattering states the boundary conditions to be imposed to the $\{u_\nu\}$ will be discussed in the next Section.

The first step in the implementation of an HA calculation consists in obtaining the adiabatic basis elements and the associated adiabatic potentials, solutions of eq. (9), for a number of values of ρ . Among several available techniques we have chosen to use a variational approach, by expanding the functions $\{\Phi_\nu^{LST\Pi}\}$ onto a set of Hyperspherical Harmonics (HH) of size N_H . In order to define a basis set with the desired properties under particle permutation, we combine opportunely hyperspherical polynomials based on different set of Jacobi coordinates [8]. The expansion for $\Phi_\nu^{LST\Pi}$ reads:

$$\Phi_\nu^{LST\Pi} = \sum_{kl}^{N_H} D_{kl}^\nu(\rho) |kl, LST\Pi\rangle, \quad (13)$$

with the basis element given, for $L = 0$, by

$$|kl, 0ST\Pi\rangle = \sum_{i=1}^3 \left[{}^{(2)}P_k^{l,l}(\Omega_i) \otimes T_i \otimes S_i \right], \quad (14)$$

where S_i (T_i) indicates the coupling of particles jki to a state of total spin S (total isospin T), and the hyperspherical polynomial is written as (see for instance Ref. [12, 13] for more details):

$${}^{(2)}P_k^{l,l}(\Omega) = N_{kl} (1 - z^2)^{(l/2)} P_k^{l+1/2, l+1/2}(z) P_l(\mu) \quad , \quad (15)$$

where $P_k^{\alpha,\beta}$ is a Jacobi polynomial, P_l is a Legendre polynomial and N_{kl} is a normalization factor. The HH so defined are eigenfunctions of the grand-angular operator,

$$G^2|kl, 0ST\Pi\rangle = K(K+4)|kl, 0ST\Pi\rangle, \quad (16)$$

where K is the grand-angular quantum number ($K = 2k + 2l$).

The unknown coefficients $\{D_{kl}'\}$ in eq. (13), and the adiabatic potential $\{U_\nu\}$ are obtained as the eigenvectors and eigenvalues, respectively, of the following generalized eigenvalue problem

$$\sum_{kl}^{N_H} \langle k'l', LST\Pi | \mathcal{H}_\Omega - U | kl, LST\Pi \rangle D_{kl} = 0. \quad (17)$$

In practical calculations the size N_H of the HH basis set is increased until convergence is reached for the desired number N_A of adiabatic potentials $\{U_\nu\}$. However, it is well known that the convergence becomes harder to achieve the larger the value of ρ . The reason for this behavior is connected to the specific properties of the HA basis set at large ρ . Namely, the lowest adiabatic potentials tend to the binding energies of all possible two-body subsystems, and the associated HA basis elements to the two-body wavefunctions, opportunely normalized. The HH expansion is not optimal for reproducing wavefunctions with similar characteristics, which become the more localized the larger ρ . This convergence problem can be further enhanced by the presence of a hard core repulsion in the two-body potential. If the calculation is to be limited to the three-body bound states, and in absence of very extended ones such as the Efimov states, the limited radius of convergence of the HH expansion does not constitute a problem. When the calculation is extended to the continuum energy region, however, the accurate determination of the adiabatic curves and functions at very large ρ becomes essential for the convergence of the results. In order to overcome this problem Blume and co-workers [2] advocate the use of splines, which at large ρ converge significantly faster than the HH. Alternatively, when ρ is much larger than the range of the two-body interaction, approximations for the HA basis elements and potentials can be obtained by solving a non-homogeneous one-dimensional differential equation. A brief illustration of this second approach is summarized below, based on the work of Nielsen and co-workers [1]. Let us start from the definition of the reduced amplitudes ϕ_ν

$$\Phi_\nu^{LST\Pi} = \sum_{i=1,3}^3 \Phi_\nu^{(i)} = \sum_{i=1}^3 \frac{\phi_\nu(\theta_i, \rho)}{\cos \theta_i \sin \theta_i}. \quad (18)$$

each one having the set of quantum numbers $LST\Pi$. They are the solutions of the Faddeev equations, that for s -wave potentials read

$$\left(-\frac{\hbar^2}{2m\rho^2}\frac{d^2}{d\theta_i^2} + V(\sqrt{2}\rho\cos\theta_i) - \lambda_\nu(\rho)\right)\phi_\nu(\rho, \theta_i) = -\cos\theta_i\sin\theta_i V(\sqrt{2}\rho\cos\theta_i) \int_{-1}^1 d\mu_i (\Phi_\nu^{(j)} + \Phi_\nu^{(k)}) \quad (19)$$

where $\lambda_\nu(\rho) = U_\nu(\rho) - 4\hbar^2/(2m\rho^2)$. Defining $r_0 = \sqrt{2}\rho\cos\theta_0$ the range of the (short-range) potential, we observe that, for large values of ρ , the potential $V(\sqrt{2}\rho\cos\theta_i)$ can be considered different from zero only for values of θ_i in the interval $\theta_0 \leq \theta_i \leq \pi/2$, which is the smaller the larger ρ . Accordingly, the above equation has two regimes depending the values of θ_i . It is homogeneous for $\theta_i < \theta_0$. For values in which the potential is not zero we have to evaluate the non-homogeneous term which depends on the amplitudes j, k . From the relation between the different sets of Jacobi coordinates, the region of values of θ_i where V is different from zero correspond to the values $\theta_j \approx \pi/6$ and $\theta_k \approx \pi/6$. In this region each of these amplitudes is governed by the corresponding homogeneous Faddeev equation. For example, for the j -amplitude, the possible solutions depending on the value of λ_ν are

$$\begin{aligned} \phi_\nu(\rho, \theta_j) &= A \sin(k_\nu \theta_j) \quad \lambda_\nu > 0 \\ \phi_\nu(\rho, \theta_j) &= A(e^{k_\nu \theta_j} - e^{-k_\nu \theta_j}) \quad \lambda_\nu < 0 \quad , \end{aligned} \quad (20)$$

and similarly for the k -amplitude, where $k_\nu^2 = 2m|\lambda_\nu|/\hbar^2$. Replacing these expressions in the Faddeev equation (19), its asymptotic form can be obtained:

$$\left(-\frac{\hbar^2}{2m\rho^2}\frac{d^2}{d\theta^2} + V(\sqrt{2}\rho\cos\theta) - \lambda_\nu(\rho)\right)\phi_\nu(\rho, \theta) = V(\sqrt{2}\rho\cos\theta)Af(\rho, \theta) \quad (21)$$

When the equation describes a two-body bound state with a third particle far away, λ_ν is negative and tends to the two-body bound state energy. The corresponding non-homogeneous term is

$$f(\rho, \theta) = -2 \frac{e^{k(\pi/2-\theta)} - e^{-k(\pi/2-\theta)}}{k} \frac{e^{k\pi/6} - e^{-k\pi/6}}{\sin(\pi/3)}. \quad (22)$$

For positive values of λ_ν the adiabatic functions describe asymptotically three free particles and

$$f(\rho, \theta) = -\frac{8 \sin(k\pi/6)}{\sqrt{3}} \sin[k(\pi/2 - \theta)]/k. \quad (23)$$

A is a normalization constant to be determined from the solutions. The boundary conditions for the functions ϕ_ν are $\phi_\nu(\rho, 0) = \phi_\nu(\rho, \pi/2) = 0$, which determine completely the solutions of eq. (21).

In practical applications the adiabatic potentials $\{U_\nu\}$ and the HA basis elements $\{\Phi_\nu^{0ST\Pi}\}$ are obtained as solutions of eq. (17) for $\rho \leq \rho_0$ and of eq. (21) for $\rho > \rho_0$, respectively. The matching point ρ_0 needs to be chosen larger than the range r_0 of the two-body potential V . There is a zone around the matching point in which, for a sufficient large value of N_H , the solutions obtained from the HH expansion or by solving eq. (21) for each value of ν become indistinguishable from each other. In this way we link the definitions of ρ_0 and N_H as the values for which the solutions of eqs.(17) and (21) can be accurately matched. In fact, if the functions ϕ_ν obtained by solving eq. (21) are themselves expanded into the HH basis, the coefficients of this expansion can be individually matched to the equivalent coefficients obtained through solving eq. (17) for the same value of ρ .

In the following we discuss the solutions of the the system of coupled differential equations (10) in the case of bound states. The hyperradial functions $\{u_\nu^n\}$ can be expanded into normalized generalized Laguerre polynomials times and exponential function [14]:

$$u_\nu^n(\rho) = \sum_{m=0}^{N_p-1} A_{m\nu}^n L_m^{(5)}(\beta\rho) \exp[-\beta\rho/2], \quad (24)$$

where β is a non-linear parameter which can be used to improve the convergence of the expansion [15]. The coefficients $\{A_{m\nu}^n\}$ can be found by means of the Rayleigh-Ritz variational principle, whose implementation requires the solution of the following eigenvalue problem:

$$\sum_{m\nu} \langle m'\nu' | \mathcal{H} - E | m\nu \rangle A_{m\nu} = 0, \quad (25)$$

where the ortonormalized basis element $|m\nu\rangle$ is defined as

$$|m\nu\rangle = L_m^{(5)}(\beta\rho) \exp[-\beta\rho/2] \Phi_\nu^{0ST\Pi}(\rho, \Omega). \quad (26)$$

The size of the variational problem is $M = N_p \times N_A$, where N_A is the number of adiabatic basis functions retained in expansion of eq. (8), and N_p is the number of Laguerre polynomials used in expansion of eq. (24). For sake of simplicity all functions u_ν^n are expanded using the same number of Laguerre polynomials, although this is not strictly necessary. The eigenvalues $\{E_n^{(M)}\}$ ($n = 1, 2, \dots$) represent upper bounds to the eigenvalues of the Hamiltonian

problem (5) and converge towards them monotonically as M is increased. The associated set of coefficients $\{A_{m\nu}^n\}$ provide approximations to the system wavefunctions.

As it has been mentioned before, there is a complete equivalence between the two methods if they include the same number of HH functions. In fact the expansion for Ψ in eq. (8) can be written also as:

$$\Psi_n^{LST\Pi} = \sum_{kl}^{N_H} w_{kl}^n(\rho) |kl, LST\Pi\rangle, \quad (27)$$

and from eq. (13) the following relation can be obtained

$$w_{kl}^n(\rho) = \sum_{\nu}^{N_A} u_{\nu}^n(\rho) D_{kl}^{\nu}(\rho). \quad (28)$$

If N_A is set equal to N_H the matrix D_{kl}^{ν} represents a unitary transformation between the HA and HH basis sets, therefore the two expansions must produce identical sets of eigenvalues and eigenvectors. Consequently, if in a specific problem, the desired accuracy is reached using N_H HH basis functions, the use of a larger number of HH basis elements in the expansion of the adiabatic basis functions is superfluous. However, we can expect that the number of adiabatic functions N_A needed to reach the same accuracy will be $N_A \ll N_H$. This is because the HA functions have been optimized to the specific Hamiltonian problem by solving eq. (9) for each value of the hyperradius. We would like to stress the fact that the equivalence between the HH and the HA method using a tractable number N_H of HH functions applies in presence of deep bound states. When shallow bound states, as Efimov states, are present the situation changes and a direct application of the HH method encounter the problem of the inclusion of a very large number of basis states in the expansion of the wavefunction. This is related to the correct description of the adiabatic potentials in the asymptotic regime. In this case the use of the asymptotic form of the Faddeev equations given above proves to be extremely useful, as for example in the solution of three Helium atoms system [1].

III. SCATTERING OBSERVABLE CALCULATIONS

In this section we apply the HA expansion to the study of continuum states of a three-body system. The case considered will be the scattering of one particle colliding other two forming a dimer, at energies below the three-body breakup threshold. The wavefunction for the system can be written as

$$\Psi = \Psi_c + \Psi_a, \quad (29)$$

where the first term is \mathcal{L}^2 and describes the system configurations in which the three particles are all close to each other. The second term represents the solution of the Schroedinger equation in the asymptotic region in which the incident particle does not interact with the other two (the discussion will be limited to short range potentials). Moreover, we will consider the case of a two-body interaction that supports only one dimer bound state of energy E^{2b} . Accordingly, we will consider energies $E^{2b} \leq E < 0$.

The explicit form of the term Ψ_a depends on the energy E of the system. However, the particular choice of the function Ψ_a is rather arbitrary, as it can be modified by adding or subtracting any \mathcal{L}^2 function. In the following we will consider and compare two different expressions for the asymptotic function Ψ_a . Practical applications will be shown for the case of nucleon-deuteron scattering using the semi-realistic s -wave MT-III potential, as the repulsive core of the potential allows a better understanding of the numerical problems associated with the method's implementation.

A. Scattering below Break-up: Method 1

The Ψ_a term must describe the asymptotic state of the dimer plus a third particle. Therefore, the most natural choice for this term leads to building two independent and symmetrized states, that for $L = 0$, read as follows:

$$\Omega_{ST}^R = \sum_i \mathcal{N} \frac{g(r_i)}{r_i} \frac{\sin[k_y y_i]}{k_y y_i} P_0(\mu_i) |ST\rangle, \quad (30)$$

and

$$\Omega_{ST}^I = \sum_i \mathcal{N} \phi_d(r_i) \frac{\cos[k_y y_i](1 - \exp[-\gamma y_i])}{k_y y_i} P_0(\mu_i) |ST\rangle. \quad (31)$$

The distance between particle i and particles j, k forming a dimer is y_i , $\phi_d(r)$ is the dimer wavefunction of energy E^{2b} , $k_y^2 = 4m(E - |E^{2b}|)/3\hbar^2$ and \mathcal{N} is a normalization factor chosen so that

$$\langle \Omega_{ST}^R | \mathcal{H} - E | \Omega_{ST}^I \rangle - \langle \Omega_{ST}^I | \mathcal{H} - E | \Omega_{ST}^R \rangle = 1/2. \quad (32)$$

The behavior of the function Ω_{ST}^I for $y_i \rightarrow 0$ has been regularized by means of an opportune factor. The constant γ can be consider a non linear parameter of the scattering wave function. The final result should be independent of the value chosen for it but a wrong choice can slow down the convergence significantly. A reasonable choice could be $\gamma \approx \sqrt{m|E^{2b}|/\hbar^2}$.

A general scattering state is given by defining the following linear combinations

$$\Omega_{ST}^0 = u_{0R}\Omega_{ST}^R + u_{0I}\Omega_{ST}^I, \quad (33)$$

and

$$\Omega_{ST}^1 = u_{1R}\Omega_{ST}^R + u_{1I}\Omega_{ST}^I. \quad (34)$$

The term Ψ_a , having total spin S and total isospin T , can thus be written as

$$\Psi_a = \Omega_{ST}^0 + \mathcal{L}\Omega_{ST}^1 \quad (35)$$

where different choices for the matrix u can be used to define the scattering matrix \mathcal{L} [16].

Here we will use

$$u = \begin{pmatrix} i & -1 \\ i & 1 \end{pmatrix} \quad (36)$$

defining $\mathcal{L} \equiv S$ -matrix and $\det u = 2i$. Another possible choice used here corresponds to $u_{0R} = u_{1I} = 1$ and $u_{1R} = u_{0I} = 0$ defining $\mathcal{L} \equiv \mathcal{R}$, the reactance matrix. The two representations are related as

$$\mathcal{S} = (1 + i\mathcal{R})(1 - i\mathcal{R})^{-1}. \quad (37)$$

This identity holds for the exact matrices therefore it can be used as a check of the accuracy of the calculation by comparing the results using both schemes.

At energies below the three-body breakup, the Ψ_c term is \mathcal{L}^2 . Accordingly it can be represented by means of an expansion in the same \mathcal{L}^2 basis used for bound states, namely

$$\Psi_c = \sum_{m\nu} A_{m\nu} |m\nu\rangle \quad (38)$$

From the above definitions we can construct the scattering state as

$$\Psi = \sum_{m\nu} A_{m\nu} |m\nu\rangle + \Omega_{ST}^0 + \mathcal{L}\Omega_{ST}^1 \quad (39)$$

The solution of a scattering problem at a given energy requires the determination of the amplitude \mathcal{L} and the linear coefficients $A_{m\nu}$. To this aim we make use of the Kohn variational principle [16] that can be written as

$$[\mathcal{L}] = \mathcal{L} - \frac{2}{\det u} \langle \Psi^* | \mathcal{H} - E | \Psi \rangle. \quad (40)$$

The numerical implementation of the variational principle leads to a first order approximation of the amplitude \mathcal{L} obtained through the solution of a linear system of equations of size $M + 1$, where M is the size of the basis set for the expansion of the core part of the wavefunction. If we define an array of unknowns $(\{A_{m\nu}\}, \mathcal{L})$ of dimension $M + 1$, the linear system can be written as:

$$\begin{pmatrix} H_{m'\nu',m\nu} & H_{m'\nu',\Omega^1} \\ H_{\Omega^1,m\nu} & H_{\Omega^1,\Omega^1} \end{pmatrix} \begin{pmatrix} A_{m\nu} \\ \mathcal{L} \end{pmatrix} = \begin{pmatrix} -H_{m'\nu,\Omega^0} \\ \frac{1}{4}(\det u - 2H_{\Omega^1,\Omega^0} - 2H_{\Omega^0,\Omega^1}) \end{pmatrix}, \quad (41)$$

where $H_{x',x}$ stands for the matrix element

$$H_{x',x} = \langle x'^* | \mathcal{H} - E | x \rangle. \quad (42)$$

The second order estimate for \mathcal{L} is then given by

$$\mathcal{L}^{2nd} = \mathcal{L}^{1st} - \frac{2}{\det u} \langle \Psi^{1st*} | \mathcal{H} - E | \Psi^{1st} \rangle, \quad (43)$$

where Ψ^{1st} is the wavefunction obtained solving the linear system of eq.(41).

Let us now discuss in more detail the structure of eq. (41). The top left part of the coefficient matrix, of dimension $M \times M$ contains the matrix elements used for the bound state calculation when the scattering state has the same quantum numbers as the bound state (compare it to eq. (25)). Otherwise specific states $|m\nu\rangle$ having proper quantum numbers have to be constructed. The additional matrix elements needing to be computed are those between the \mathcal{L}^2 basis functions and the scattering functions, and among the scattering functions themselves, for a total of $2M + 4$ different terms. The number of such extra terms grows linearly with the basis set size, and due to the functional form of Ω_{ST}^0 and Ω_{ST}^1 , they need to be calculated at every different choice of the system energy E .

The application discussed above employ the HA basis in the expansion of the $\mathcal{L}^2 \Psi_c$ term. Alternatively, Ψ_c could also have been expanded in terms of sole HH functions as

$$\Psi_c = \sum_{mkl} A_{mkl} |mkl\rangle, \quad (44)$$

where we have defined the ket

$$|mkl\rangle = L_m^{(5)}(\beta\rho) \exp[-\beta\rho/2] \otimes |kl, 0ST\Pi\rangle. \quad (45)$$

After including a sufficient number of Laguerre polynomials, both expansions, in terms of HH or HA functions, are equivalent leading to the same value of \mathcal{L} . Example of this equivalence will be shown and discussed in the next Section.

B. Scattering below Break-up: Method 2

An alternative approach considered is represented by a direct solution of eq. (10) which represents a different form of the three-body Schroedinger equation. The bound state solutions have been discussed in Sect.II, and here we will discuss the scattering solutions below three-body breakup: $E^{2b} \leq E < 0$. For this purpose it is important to determine the boundary conditions to be imposed to the functions $\{u_\nu^E(\rho)\}$. Firstly, let us observe that at very large ρ the only open channel in the system of eqs.(10) is the lowest one, and that the system uncouples:

$$\left(-\frac{\hbar^2}{2m}T_\rho + U_1 - E + B_{11}\right) u_1 = 0. \quad (46)$$

At $\rho = 0$ corresponds $u_1(0) = 0$, whereas the boundary conditions at large ρ depend on the specific asymptotic forms of the hyperradial potentials $U_1(\rho)$ and of the terms $B_{11}(\rho)$. A detailed study of their asymptotic expressions will be object of a forthcoming publication [17]. For the purpose of this work it suffices to say that

$$\left(-\frac{\hbar^2}{2m}T_\rho + U_1 - E + B_{11}\right) u_1 \rightarrow \left(\frac{d^2}{d\rho^2} + k_\rho^2 + o(\rho^{-3})\right) (\rho^{5/2}u_1), \quad (47)$$

where the wavenumber k_ρ is defined from the relation:

$$E = E^{2B} + \frac{\hbar^2}{2m}k_\rho^2. \quad (48)$$

The boundary conditions associated with u_1 thus are

$$u_1(0) = 0, \quad \lim_{\rho \rightarrow \infty} u_1(\rho) \rightarrow \tilde{u}_1 = \frac{\sin(k_\rho \rho)}{\rho^{5/2}} + \tan \delta \frac{\cos(k_\rho \rho)}{\rho^{5/2}}, \quad (49)$$

all other $u_\nu \rightarrow 0$ sufficiently fast, as $\rho \rightarrow \infty$. Furthermore, the lowest adiabatic function $\Phi_1^{0ST\Pi}(\rho, \Omega) \rightarrow \rho^{3/2}\phi_d(r)|ST\rangle$ at very large values of ρ [5]. Therefore, the asymptotic behavior of the scattering wave function in terms of the adiabatic basis results:

$$\Psi = \sum_\nu u_\nu(\rho)\Phi_\nu^{0ST\Pi}(\rho, \Omega) \rightarrow \phi_d(r) \left[\frac{\sin(k_\rho \rho)}{\rho} + \tan \delta \frac{\cos(k_\rho \rho)}{\rho} \right] |ST\rangle. \quad (50)$$

In the limit $\rho \rightarrow \infty$ the relation $k_y y \approx k_\rho \rho$ holds as r is constrained by the finite size of the dimer wavefunction, therefore $r/\rho \ll 1$. Consequently eq. (50) represent the asymptotic limit of $\Omega_{ST}^R + \tan \delta \Omega_{ST}^I$, for $\rho \rightarrow \infty$. The full equivalence between the above expression for the asymptotic wavefunction and that one given by eqs. (30,31) can be established by

noticing that the \tilde{u}_1 constitutes the leading term in the expansion of Ω_{ST}^R and Ω_{ST}^I in terms of the small parameter r/ρ [6], which yields

$$\langle \Omega_{ST}^R | \Phi_1 \rangle \approx \frac{\sin[k_\rho \rho]}{\rho^{5/2}} + \mathcal{O}(\rho^{-7/2}), \quad (51)$$

and

$$\langle \Omega_{ST}^R | \Phi_\nu \rangle \approx \frac{\cos[k_\rho \rho]}{\rho^5} + \mathcal{O}(\rho^5) (\nu > 1). \quad (52)$$

and a similar expansion yields for Ω_{ST}^I . From the above discussion, we can define an alternative asymptotic term Φ_a as combination of the following functions:

$$\Omega_{\rho,ST}^R = \sqrt{\frac{m}{2\hbar^2 k_\rho}} (1 - \exp[-\gamma\rho])^\eta \frac{\sin[k_\rho \rho]}{\rho^{5/2}} \Phi_1(\Omega, \rho), \quad (53)$$

and

$$\Omega_{\rho,ST}^I = \sqrt{\frac{m}{2\hbar^2 k_\rho}} (1 - \exp[-\gamma\rho])^\eta \frac{\cos[k_\rho \rho]}{\rho^{5/2}} \Phi_1(\Omega, \rho), \quad (54)$$

where the factor $(1 - \exp[-\gamma\rho])^\eta$ is introduced as usual to regularize the behavior of the functions for $\rho \rightarrow 0$ (in practical calculations we have set $\eta = 4$), and the functions are normalized as in eq. (32). The same approach as in the previous Section can now be applied where. Accordingly the scattering wave function can be written as

$$\Psi = \sum_{M\nu} B_{m\nu} |m\nu\rangle + \Omega_{ST}^0 + \mathcal{S} \Omega_{ST}^1 \quad (55)$$

where the asymptotic part is now given in terms of $\Omega_{\rho,ST}^R$ and $\Omega_{\rho,ST}^I$, and the core part Ψ_c is expanded onto the HA basis times a set of \mathcal{L}^2 functions $u_\nu(\rho)$. We can refer to this expansion as HA2.

This approach is justified as the neglected terms in the r/ρ expansion of Ω^R and Ω^I do not carry flux and can be incorporated into the unknown term Ψ_c . The approximated expression for the term Ψ_a allows to speed up the calculation significantly as there is no need to calculate the overlap integrals between the HA basis functions and the asymptotic functions as in eq. (41). On the other hand, its implementation suffers from the following problems. At intermediate distance the expansion on r/ρ of the asymptotic functions converges very slowly, resulting in a large number of HA functions which need to be taken into account. At large ρ , the implementation of the functions of eqs. (30,31) results in a very awkward behavior of the \mathcal{L}^2 term Ψ_c . Continuing the expansion of eq. (51), for instance, it is possible to show that the next term is $\cos[k_\rho \rho]/\rho^{7/2}$, which imposes the asymptotic behavior that

the function u_1 has to reproduce. This particular functional form is very slow decaying, and it is particularly hard to reproduce with a polynomial expansion. This problem is further enhanced by the presence of oscillations associated with cosine and sine terms.

In order to solve the linear system (41) taking into account the oscillatory behavior of the hyperradial functions for large ρ values, we have implemented a Discrete Variable Representation (DVR) scheme [18] rather than the standard variational approach. In a previous work [19] we have shown how to combine the variational Kohn principle with a DVR scheme, for the case of a two-body system, which corresponds to a single one-dimensional differential equation. In this work we have a set of N_A one-dimensional coupled differential equations. Therefore we define a $(N_A M + 1) \times (N_A M + 1)$ unitary transformation matrix \mathcal{U} which is a direct product of $N_A + 1$ matrices

$$\mathcal{U} = \mathcal{U}^{1d} \otimes \mathcal{U}^{1d} \otimes \dots \otimes 1, \quad (56)$$

where \mathcal{U}^{1d} is a $M \times M$ unitary matrix associated to a customary one-dimensional DVR of size $N_{DVR} = M$ built in ρ :

$$\mathcal{U}_{ij}^{1d} = L_i^{(5)}(t_j) \exp[-t_j/2] \sqrt{w_j}, \quad (57)$$

where t_j and w_j are the appropriate quadrature points and weights. By mean of a parameter β , the end quadrature point $t_{N_{DVR}}$ can be associated to different physical values ρ_{max} , by setting $t_j = \beta \rho_j$. In this fashion we can constrain the quadrature points to be distributed between 0 and ρ_{max} .

IV. NUMERICAL APPLICATIONS

In order to illustrate the method outlined in the previous Sections we present two applications to the $n - d$ system in a quartet state ($S = 3/2$). The potential energy of the system is taken as the sum of three pairwise potentials. We consider the MT-III interaction V_{MT-III} for which benchmarks results exist in the literature [9]. It reads:

$$V_{MT-III}(r) = (1438.72 \exp[-3.11 r] - 626.885 \exp[-1.55 r]) / r. \quad (58)$$

To make contact with the results of Ref. [6], we have also used the Gaussian potential (named V_G):

$$V_G(r) = -66.327 \exp[-(0.64041 r)^2], \quad (59)$$

For both potentials we assume nuclear distances in fm and energies in MeV. The nucleon mass used is such that $\hbar^2/m = 41.47 \text{ MeV fm}^2$. Furthermore, we consider both potentials as acting only on the $l = 0$ two-body partial wave.

The potential V_G supports one deuteron bound state, with zero angular momentum, of energy $E_{2b} = -2.22448 \text{ MeV}$. The zero-energy scattering length is $a_s = 5.4208 \text{ fm}$, whereas for the MT-III potential the values are $E_{2b} = -2.23069 \text{ MeV}$, and $a_s = 5.5132 \text{ fm}$.

For the potential V_G we consider the three-body system with quantum numbers $\Pi = a$, $T = 1/2$ and $S = 1/2$, whereas for V_{MT-III} $\Pi = a$, $T = 1/2$ and $S = 3/2$. As the potentials are projectors on s -wave, the index l in eq. (14) is restricted to the value $l = 0$, and the index k can take the values $k = 0, 2, 3, 4, 5, \dots, \infty$ in the first case and $k = 1, 2, 3, 4, 5, \dots, \infty$ in the second case.

A. Bound states

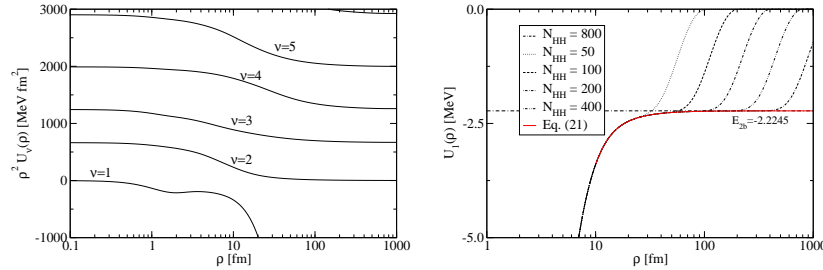


FIG. 1: The top panel shows the lowest adiabatic curves $U_\nu(\rho)$ for different values of ρ . In order to display the behavior at large ρ the curves are multiplied by a factor ρ^2 . The lowest curve thus tends to $E_{2b}\rho^2$, and the others to the spectrum $\hbar^2 K(K+4)/m$, with $K = 0, 2, 3, 4, \dots$ for $\nu = 2, 3, 4, 5, \dots$. The bottom panel shows the convergence of the lowest adiabatic curve $U_1(\rho)$ as a function of the number of HH used in the expansion of eq. (13). The asymptote at $E_{2b} = -2.2245 \text{ MeV}$ is plotted for comparison.

Figure 1 shows, in the upper panel, the lowest adiabatic curves $U_\nu(\rho)$ calculated for the V_G potential. In order to highlight their asymptotic behavior, the curves have been multiplied by a factor ρ^2 . The lowest curve $U_1(\rho)$ thus tends to the deuteron energy times ρ^2 , whereas the upper curves tend to the free HH spectrum, that is $4k(k+2)\hbar^2/m$ with

$k = 0, 2, 3, 4, 5, \dots$ for $\nu = 2, 3, 4, 5, 6, \dots$. The value $k = 1$ is not allowed as there is no completely symmetric HH with $k = 1$ and $l = 0$. Subsequently, the adiabatic function $\Phi_1(\rho, \Omega)$ tends to the deuteron wavefunction, whereas Φ_ν , $\nu > 1$, to the HH functions, with the appropriate normalization factors. The lower panel shows the convergence of the lowest curve $U_1(\rho)$ as a function of the number of HHs employed in the expansion of eq. (13). It shows that the larger ρ becomes, the larger the expansion basis must be in order to properly describe the function Φ_1 . In practice, the radius of convergence of expansion (13) increases rather slowly when the basis set size is increased. The reason for this behavior is that when ρ is increased the function Φ_1 becomes more and more localized in the hyperangular phase-space, therefore its description by means of the HH requires a larger and larger basis set size. This behavior is not connected with any particular feature of the potential used in this specific calculation but it can be considered a general one, as it is induced by the geometric localization of the deuteron wavefunction in connection with the HH expansion. The thick curve is the solution of eq. (21) starting at $\rho = 20$ fm. For large values of ρ , the corresponding eigenvalue reproduces the two-body binding energy E_{2b} .

The description of a three-nucleon bound state using a central potential has to been taken as a homework problem and preliminary to check the usefulness of the HA basis to treat scattering states, in comparison to the HH expansion. The V_G potential predicts two bound states in the three-body system, a very deep ground state and a very shallow excited state. Table I reports the convergence patterns for the upper bounds E_1^N and E_2^N to the two bound states supported by the potential V_G , as a function of the number N of HA and HH basis elements. The HA functions were expanded in 80 HH functions which is the number required for the HH expansion to describe accurately the deep and shallow bound states. The number of HH functions necessary to obtain a full convergence of the energy for the deep bound state is much smaller, around 10 functions. The most striking feature to be observed in the table is the much rapid convergence of the HA basis expansion compared to the HH. Not only full convergence can be achieved with a basis which is one order of magnitude smaller, but already the inclusion of only one basis element yields an energy for the excited state within 90% of its converged value.

n=1			n=2		
N	HH	HA	N	HH	HA
1	-21.5808	-22.0520	1	0.0620	-2.3484
2	-21.9567	-22.0850	4	-0.9576	-2.3627
3	-22.0694	-22.0873	10	-2.0348	-2.3632
4	-22.0805	-22.0874	20	-2.3036	-2.3632
5	-22.0852	-22.0874	30	-2.3474	-2.3632
6	-22.0869	-22.0874	40	-2.3582	-2.3632
7	-22.0872	-22.0874	50	-2.3615	-2.3632
8	-22.0873	-22.0874	60	-2.3626	-2.3632
9	-22.0874	-22.0874	70	-2.3631	-2.3632
10	-22.0874	-22.0874	80	-2.3632	-2.3632

TABLE I: Patterns of convergence for the three-nucleon bound states obtained with the V_G potential, as a function of the number N of hyperangular basis functions included in the expansion. The HA basis elements were calculated with 80 HH, $\beta = 1.6 \text{ fm}^{-1}$, and 33 Laguerre polynomials were employed in the expansion of eq. (24). Note the different scales for the ground and excited state patterns of convergence.

B. Scattering States

In the following, results obtained combining the HA basis expansion with the expressions of eqs.(30,31) are given and will be referred to as HA1. Table II reports the full patterns of convergence of the $L = 0, S = 3/2$ MT-III phase shift δ , at $E_{cm} = 1 \text{ MeV}$, as a function of the number of Laguerre polynomials N_p used in expanding the hyperradial functions in eq. (38) and the number N_A of adiabatic channels included. The HA functions have been calculated using 200 HH functions. This number of HH functions is sufficient to accurately describe the phase shifts below the three-body breakup. From the table it can be seen that the convergence requires a rather high number of HA basis elements, more than 100, whereas 12 Laguerre polynomials are enough to achieve final convergence.

In order to analyze deeply the pattern of convergence, in Table III results obtained by means of the HH expansion [20] are compared to those obtained with the HA approach. In

$N_p \backslash N_A$	20	40	60	80	120	160	200
5	-55.974	-55.912	-55.902	-55.898	-55.897	-55.896	-55.896
9	-55.937	-55.879	-55.870	-55.867	-55.865	-55.864	-55.864
13	-55.932	-55.878	-55.868	-55.865	-55.864	-55.863	-55.863
17	-55.934	-55.878	-55.868	-55.865	-55.863	-55.863	-55.863
21	-55.932	-55.878	-55.868	-55.865	-55.864	-55.863	-55.863
25	-55.933	-55.878	-55.868	-55.865	-55.864	-55.863	-55.863
29	-55.932	-55.878	-55.868	-55.865	-55.864	-55.863	-55.863
33	-55.931	-55.878	-55.868	-55.865	-55.864	-55.863	-55.863

TABLE II: Convergence of the phase-shift δ in function of the number of Laguerre polynomials N_p (see eq. (24)) and of the size N_A of the HA basis set, at an incident energy of $E = 1.00$ MeV. The HA basis is calculated with 200 HH elements. The non-linear parameter was fixed to $\beta = 1.9$ fm $^{-1}$.

each row of the table N_A indicates the number of HH functions used in the calculation and the number of HA functions used calculated using 200 HH functions. As already pointed out, for the special case of $N_H = N_A$ the two expansions are equivalent and the results become identical, provided that a sufficiently high number of Laguerre polynomials is employed to describe the $\{u_\nu(\rho)\}$ set of functions. Therefore the equivalence can be seen in the last row of the table in correspondence with $N_A = 200$ (in some cases the equivalence is reached already at $N_A = 160$). For the case of $E = 2.00$ MeV, two patterns of convergence are shown for two different HA bases, obtained with 120 HH and 200 HH, respectively. Here the equivalence can be seen also at $N_A = 120$. In this energy range there is little difference in the results obtained with the two bases, for example when 20 or 40 HA basis elements are employed. To be noticed that the results shown in Table III present a different pattern of convergence with respect to the ones given in Table 2 of Ref [20]: the reason is that in the previous paper the S -matrix representation was chosen for the matrix u , whereas in this work the R -matrix was preferred. The two choices are equivalent and lead, once convergence is achieved, to the same results. We can conclude that although there is some improvement, the table shows that the convergence is not speed up significantly by transforming the HH basis into the HA basis. This suggests that the HA basis does not provide as an optimized basis for the

scattering problem as it does for the bound state problem.

	0.20 MeV		1.00 MeV		2.00 MeV	
N_A	HH	HA1	HH	HA1	HH	HA1
					120	200
20	-28.263	-28.312	-56.913	-55.931	-70.741	-71.594 -71.597
40	-28.201	-28.299	-55.948	-55.878	-71.701	-71.501 -71.500
60	-28.306	-28.295	-55.922	-55.868	-71.508	-71.485 -71.483
80	-28.296	-28.294	-55.872	-55.865	-71.483	-71.480 -71.478
120	-28.294	-28.294	-55.865	-55.864	-71.476	-71.476 -71.475
160	-28.294	-28.294	-55.863	-55.863	-71.474	- -71.474
200	-28.294	-28.294	-55.863	-55.863	-71.474	- -71.474

TABLE III: Convergence of the phase-shift δ at three different energies below break-up threshold for the MT-III potential, in function of the size N of the basis. The patterns of convergence for the HH and HA1 methods are shown for comparison. The HA basis was calculated employing 200 HH basis elements. For $E = 2.00$ MeV the calculation with 120 HH basis elements is also shown. All calculations employed 33 Laguerre polynomials (see Table II), and $\beta = 1.9 \text{ fm}^{-1}$.

Table IV shows the convergence pattern for the phase-shift at $E=1.00$ MeV, obtained using the HA2 expansion for the asymptotic term. As anticipated in the previous Section, in order to obtain stability in the phase shift, we have employed a much larger and finer hyperradial grid, consisting of 4153 points, distributed up to $\rho = 2000$ fm. At the same time the HA basis set and associated eigenvalues were obtained with a bigger number, up to 2000, of HH basis functions, or by solving the asymptotic differential eq.(21) for $\rho \geq \rho_0$ ($\rho_0 = 40$ fm). This calculation has been performed using the Laguerre polynomials as an expansion basis for the hyperradial functions. As anticipated, the polynomials are not an appropriate choice to reproduce the long range oscillatory behavior of the hyperradial functions. This can be seen from the poor convergence pattern in terms of N_p as the number of HA functions increases. For $N_A > 8$ more than 100 polynomials are necessary. Furthermore, the convergence pattern is also poor relative to the increase of the number of HA basis elements. Differences with results of Table II are remarkable.

$N_p \backslash N_A$	4	8	16	24	32	36	40
21	-57.753	-57.231	-57.063	-57.037	-57.230	-57.028	-57.027
41	-57.638	-56.915	-56.581	-56.511	-56.489	-56.484	-56.480
61	-57.628	-56.868	-56.456	-56.348	-56.310	-56.300	-56.293
81	-57.627	-56.858	-56.414	-56.281	-56.228	-56.214	-56.204
101	-57.626	-56.855	-56.399	-56.251	-56.188	-56.169	-56.156
121	-57.626	-56.853	-56.393	-56.237	-56.166	-56.145	-56.129

TABLE IV: Convergence of the phase-shift δ , using the HA2 method, in function of the number of Laguerre polynomials N_p (see eq. (24)) and of the size N_A of the HA basis set, at an incident energy of $E = 1.00$ MeV. The HA basis is calculated with 2000 HH elements. The non-linear parameter was fixed to $\beta = 1.9 \text{ fm}^{-1}$.

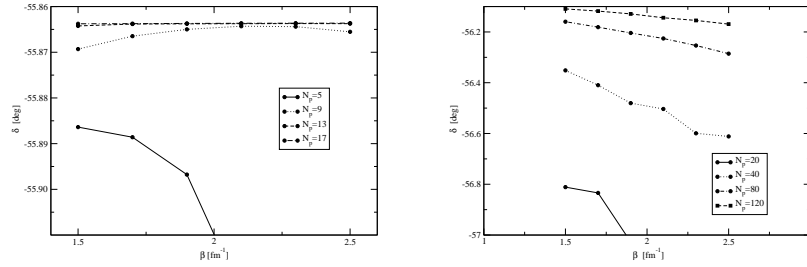


FIG. 2: The phase-shift δ in terms of different choices of the non-linear parameter β and of the size of the expansion in Laguerre polynomials. The top panel shows the convergence for expansion HA1, and the bottom panel for expansion HA2. Note the different scales on the y -axis of the two graphs.

Figure 2 shows the effect on the phase-shift of varying the non-linear parameter β . The upper panel shows results for the HA1 expansion, whereas the lower panel refers to the HA2 expansion. Different sizes of the Laguerre basis are shown. In principle, for a complete basis set, that is $N_p = \infty$, there should be no effect in varying the parameter β . When the basis set is finite, the stability of the result, in this case the phase-shift, with respects to changes of β is a measure of the completeness of the expansion. In particular, by comparing the upper and lower panels, one can see that the HA1 polynomial expansion of the functions $u_\nu(\rho)$ is much more effective than for the case HA2 (also note the different scales of the

$\rho_{\max} \backslash N_{DVR}$	100	150	200	250	300	350	
						1 st	2 nd
200	-56.179	-56.161	-56.159	-56.159	-56.159	-56.161	-56.160
400	-56.124	-56.100	-56.095	-56.093	-56.092	-56.091	-56.092
600	-56.096	-56.089	-56.085	-56.084	-56.084	-56.085	-56.083
800	-56.119	-56.089	-56.084	-56.083	-56.082	-56.080	-56.081
1000	-56.162	-56.087	-56.082	-56.081	-56.081	-56.082	-56.081
1200	-56.149	-56.088	-56.082	-56.081	-56.081	-56.082	-56.081
1400	-56.106	-56.084	-56.082	-56.081	-56.081	-56.077	-56.080
1600	-56.154	-56.090	-56.082	-56.081	-56.081	-56.082	-56.080

TABLE V: Convergence of the phase-shift δ at $E = 1.00$ MeV, using the HA2 method, for the MT-III potential, as a function of the number N_{DVR} of DVR points employed, and of the last grid point ρ_{\max} . Convergence is shown for the second order estimate of δ for all values of M, but the last, where both first and second order are shown.

y -axis). In the first case, the expansion with 17 polynomials is completely unaffected by changes in β , whereas in the second case even a basis set as large as 120 polynomials yields significantly different results with different choices of β , indicating that the result is far from convergence.

In order to circumvent this problem we use the DVR technique in the hyperradius variable. Table V shows the convergence, in terms of different choices of ρ_{\max} and the number of DVR points employed, of a case calculation, with 40 adiabatic functions, for the MT-III potential and $E = 1.00$ MeV. For the biggest case ($N_{DVR} = 350$), we show both the first and second order values of the phase-shift obtained by using the Kohn Variational Principle. In order to obtain a good convergence of the second order value it is important that the integral in eq. (43) is calculated with a very high numerical accuracy. The hyperradial grid used in the calculation consists in more than 4000 grid points up to $\rho = 2000$ fm. The use of the DVR technique allowed for stable results in terms of the hyperradial expansion. The use of 350 DVR points is equivalent to a calculation with 350 Laguerre polynomials which in general is much more involved to be carried. However the number $N_A = 40$ of HA functions used in this calculation is not enough to well describe the phase shift. At $E=1.00$ MeV the HA1

method as well as the HH method predict $\delta = -55.863$ degrees to be compared to the result of the HA2 method, $\delta = -56.081$ degrees, using $N_A = 40$. In order to have an stable result for δ using the HA2 method, the value $N_A = 120$ has to be considered and $N_{DVR} > 350$ since the number of DVR points has to be increased as N_A increases. The dimension of the HA2 problem is $N_A \times N_{DVR}$ and is clear that very soon the problem becomes computationally unsustainable, unless exceptional computational resources are considered.

N_A	0.20 MeV		1.00 MeV		2.00 MeV	
	HA1	HA2	HA1	HA2	HA1	HA2
4	-28.364	-29.065	-56.136	-57.625	-72.344	-71.988
8	-28.340	-28.739	-56.038	-56.852	-71.965	-71.871
12	-28.328	-28.604	-55.984	-56.545	-71.770	-71.437
16	-28.319	-28.532	-55.947	-56.385	-71.660	-71.210
20	-28.312	-28.487	-55.922	-56.286	-71.597	-71.070
24	-28.308	-28.456	-55.906	-56.218	-71.558	-71.975
28	-28.304	-28.434	-55.895	-56.169	-71.534	-71.907
32	-28.302	-28.417	-55.888	-56.133	-71.518	-71.855
36	-28.300	-28.404	-55.882	-56.104	-71.507	-71.815
40	-28.299	-28.394	-55.877	-56.081	-71.500	-71.783
Table III	-28.294		-55.863		-71.474	

TABLE VI: Patterns of convergence for the two different choice of the asymptotic term, in terms of the number N_A of HA basis elements, at three different energies. The MT-III potential has been used. The last row reports the converged values from Table III. The columns refers to a choice of $\beta = 1.9 \text{ fm}^{-1}$ for HA1, and $\rho_{max} = 1200 \text{ fm}$ for the HA2 expansion. Moreover, the HA1 values are associated to a calculation with 200 HH, whereas the HA2 to a calculation with 2000 HH. The HA2 results have been obtained with the DVR scheme.

Table VI compares the convergence patterns for δ at three different energies for the two suggested choices for the asymptotic term Ψ_a , namely the one in eqs. (30,31), referred to as HA1, and the one in eqs. (53,54), referred to as HA2, in terms of the number N_A of adiabatic channels. Due to the very large basis sets required to obtain convergence with the HA2 term, the pattern of convergence is limited to few channels, less than required to

obtain a full convergence. The last row reports the converged values from Table III. It is possible to see that the expansion HA1 converges faster towards the final number, whereas expansion HA2 moves rather slowly. The reason is the difference in the treatment of the asymptotic wavefunction. In the HA1 method, as well as in the HH method, the asymptotic configuration described by Ψ_a is reached at intermediate distances. Conversely, in the HA2 the the configuration described by Ψ_a is reached at much larger values of ρ . Furthermore, at intermediate distances, in order to reproduce the correct behavior a big number of HA functions are needed.

The following figures present important characteristics of the hyperradial functions used in the expansion HA2.

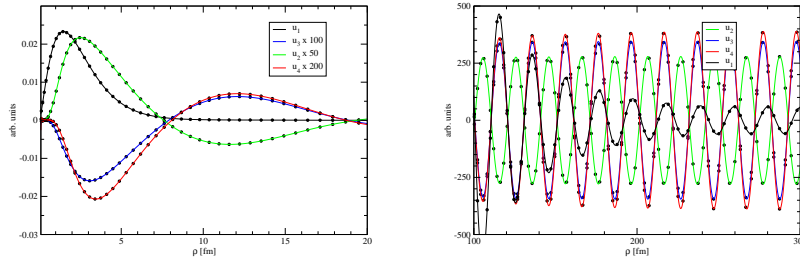


FIG. 3: The functions $u_\nu(\rho)$ ($\nu = 1, 2, 3, 4$) at $E = 2.00$ MeV. The top panel shows the short-range region. Some of the functions were magnified by the factor shown in the legend. The circles represent the DVR amplitudes at the DVR grid points. The lower panel shows the long range region. In order to highlight the asymptotic behavior of each function, u_1 is multiplied by $\rho^{7/2}$, and u_2 , u_3 and u_4 by ρ^5 . In the bottom panel u_1 is also magnified by a factor 50000.

Fig. 3 shows the functions $u_\nu(\rho)$ calculated with $N_A = 4$, $N_{DVR} = 300$ and $\rho_{max} = 1200$ fm. The dots indicate the DVR amplitudes at the DVR points, whereas the lines represent the $u_\nu(\rho)$ functions obtained by back-transforming to the original polynomial basis. The top panel displays the short-range region ($0 \leq \rho \leq 20$ fm), where the function u_1 is predominant. The bottom panel shows a part of the long-range region ($100 \leq \rho \leq 300$ fm). Here the situation is drastically different, and the functions u_2 , u_3 and u_4 have a much larger amplitude than u_1 (which is magnified by a factor 50000). Also, in order to highlight the asymptotic behavior, u_1 is multiplied by $\rho^{7/2}$, and u_2 , u_3 and u_4 by ρ^5 . The most striking feature are

the oscillations present in all curves. This behavior is a consequence of the decomposition of the asymptotic configuration in terms of HA functions. This resulting peculiar long range behavior is the cause of the very slow convergence of the phase-shift shown in Tables IV, V, VI. The behavior obtained for the curves u_ν is the one expected by the analytical expansion of the asymptotic terms indicated in eqs. (51,52).

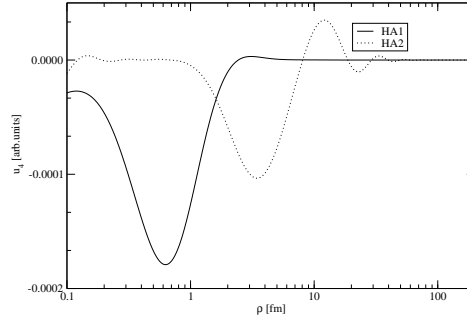


FIG. 4: The function $u_4(\rho)$ (see eq.(8)) obtained with the method HA1 (continuum line) and HA2 (dotted line). In the first case the function u_4 is short range, decaying exponentially with ρ , whereas in the second case it shows the long range oscillations.

Figure 4 compares the hyperradial function $u_4(\rho)$ obtained with method HA1 and HA2. In particular it highlights as the former is short range and exponentially decaying with ρ , compared to the latter which is oscillating as indicated in eq. (51).

As mentioned in the Introduction, in Ref. [6] the phase shift for the potential V_G has been calculated from eq. (10) in the so-called uncoupled adiabatic approximation (UUA) retaining one hyperradial function. Namely, the following equation has been solved:

$$\left[-\frac{\hbar^2}{2m} T_\rho + U_1 - E + B_{11} \right] u_1(\rho) = 0 \quad (60)$$

with the asymptotic condition $u_1(\rho) \rightarrow \sin(k\rho + \delta + 3\pi/2)$ as $\rho \rightarrow \infty$. Besides the factor $3\pi/2$, this is equivalent to the method HA2 given in the previous section taking into account one HA function.

In Figure 5 we show the phase-shift $\delta(E)$. The dots represent fully converged results obtained with the HA1 expansion, whereas the continuum line represent results obtained by

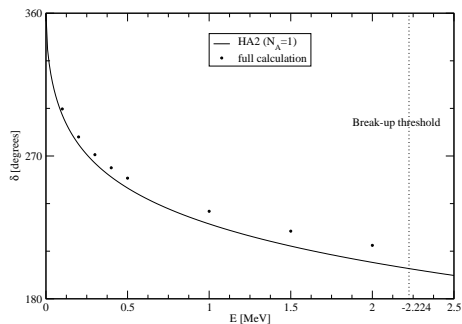


FIG. 5: Elastic deuteron-nucleon phase-shift below three-body break-up (marked by the dotted line) for the V_G potential. The full line corresponds to a calculation retaining one HA basis element, and using the HA2 method. The dots correspond to the full calculation.

including just one adiabatic function in the expansion HA2. It is possible to notice that the UUA provides a very good first order estimate of the phase-shift. However, the deviation from the complete expansion can be as big as 10%. Also notice that in Figure 5 the phase-shifts have been normalized so that $\delta(E = 0) - \delta(E = \infty) = 360$, as there are two bound trimer states.

V. CONCLUSIONS

In this paper we have investigated the capability of the HA basis to describe scattering states in a three-nucleon problem. The basis was generated from the hyperangular Hamiltonian by means of an expansion in HH functions. We have shown the complete equivalence between the adiabatic basis generated using N HH functions and the HH basis of dimension N . This equivalence provides a useful benchmark when the convergence of the quantities of interest is studied in terms of the number N_A of adiabatic functions. For example, for bound states it is well known that $N_A \ll N$ suffices for the convergence of the binding energies. One goal of this paper was to investigate whether the same relation holds for scattering states. In particular, we studied the convergence of the $L = 0$ phase shift δ corresponding to a process in which a nucleon collides a deuteron at low energies in the state $S = 3/2$. For this purpose we have used the MT-III potential.

In the calculation of the phase shift using the HA basis we have followed two different procedures. They were both based on a decomposition of the scattering wavefunction as

a sum of two terms. One term describes the configurations when the three particles are all close to each other and goes to zero as the interparticle distances increase. The second term describes the asymptotic configurations and has been regularized so that goes to zero as $y \rightarrow 0$. In the first procedure the HA basis has been used to expand the short range part of the scattering wave function. The second order estimate of the phase-shift has been obtained from the Kohn variational principle. A similar approach has been used before with the HH basis. Therefore, a detailed comparative analysis of the convergence patterns was possible. The conclusion is that the number of basis elements needed to achieve a comparable level of convergence for the phase-shift is of the same order for the two bases, that is $N_A \approx N$, which is a surprising difference with respect to what happens in bound state calculations. A possible explanation could be the following. In bound state calculations the wavefunction expansion benefits from the initial optimization performed by constructing the HA basis. Conversely, in scattering state calculations the solution of the linear system of eq.(41) requires a different short range behavior in the HA basis elements due to the presence of the terms Ω_{ST}^0 and Ω_{ST}^1 in the short distance region.

The second procedure considered was based in a direct solution of the system of equations for the hyperradial functions given in eq.(10). This method however suffers from the following complications. The hyperradial boundary conditions to be imposed are those required to reconstruct the asymptotic configuration given by the functions defined in eqs.(30,31). For very large values of ρ the boundary conditions are simple and are given by eq. (49) for the lowest function ($\nu = 1$). All other functions go to zero as $\rho \rightarrow \infty$. This means that the solution of the linear system has to be obtained over a very extended hyperradial grid. Moreover, the adiabatic potentials and functions have to be accurately known in the grid. In the present work we have solved partially the numerical difficulties associated to the solution of eq. (10) introducing a variational DVR procedure.

From the present study we can conclude that the use of the HA basis in the description of scattering states is not as advantageous as for bound states. The main drawback is that then number of basis elements required to reach convergence is not as low (in proportion) as in bound state calculations. Secondly, a number of numerical problems arise from the need of calculating the adiabatic curves and the associated basis elements at large distances. Further studies to improve the description of scattering states using the HA expansion are

at present underway.

- [1] E. Nielsen, D. V. Fedorov, and A. S. Jensen. *J. Phys. B: At. Mol. Opt. Phys*, **31** (1998) 4085–4105.
- [2] D. Blume, C. Greene, and B. D. Esry. *J. Chem. Phys.*, **113** (2000) 2145–2158.
- [3] Y. Das, H. Coelho, and M. Fabre de la Ripelle. *Phys. Rev. C*, **26** (1982) 2281.
- [4] J. Ballot and M. Fabre de la Ripelle. *Phys. Rev. C*, **26** (1982) 2301.
- [5] M. Fabre de la Ripelle, H. Fiedeldey, and S. Sofianos. *Phys. Rev. C*, **38** (1988) 449.
- [6] M. Fabre de la Ripelle. *Few-Body Systems*, **14** (1993) 1–24.
- [7] A. Kievsky, S. Rosati, and M. Viviani. *Nucl. Phys. A*, **577** (1994) 511.
- [8] A. Kievsky, M. Viviani, and S. Rosati. *Phys. Rev. C*, **56** (1997) 2987.
- [9] C. R. Chen, et al. *Phys. Rev. C*, **39** (1989) 1261.
- [10] G. L. Payne, J. L. Friar, and B. F. Gibson. *Phys. Rev. C*, **26** (1982) 1385.
- [11] V. Gusev, et al. *Few-Body Syst.*, **9** (1990) 137–153.
- [12] M. Fabre de la Ripelle. *Annals of physics*, **127** (1980) 62–125.
- [13] M. Fabre de la Ripelle. *Annals of physics*, **147** (1983) 281–320.
- [14] M. Abramovitz and I. A. Stegun. *Handbook of mathematical functions*. Dover publications, New York, (1970).
- [15] P. Barletta and A. Kievsky. *Phys. Rev. A*, **A64** (2001) 042514.
- [16] A. Kievsky. *Nuclear Physics A*, **624** (1997) 125–139.
- [17] P. Barletta and A. Kievsky. to be published.
- [18] J. C. Light and T. Carrington Jr. *Adv. Chem. Phys.*, **114** (2000) 263–310.
- [19] M. Lombardi, P. Barletta, and A. Kievsky. *Phys. Rev. A*, **70** (2004) 032503.
- [20] P. Barletta and A. Kievsky. *Few-Body Syst.*, (accepted for publication).